Preprints of the 21st IFAC World Congress (Virtual)
Berlin, Germany, July 12-17, 2020

Multi-layer model predictive control of inland waterways with continuous and discrete actuators

P. Segovia * **E. Duviella** * **V. Puig** **,***

* *IMT Lille Douai, Univ. Lille, F-59000 Lille, France (e-mail: {pablo.segovia, eric.duviella}@imt-lille-douai.fr)*
** *Research Center for Supervision, Safety and Automatic Control (CS2AC), Universitat Politècnica de Catalunya (UPC), Rambla Sant Nebridi 22, 08222 Terrassa, Spain (e-mail: vicenc.puig@upc.edu)*
*** *Institut de Robòtica i Informàtica Industrial (CSIC-UPC), c/ Llorens i Artigas 4-6, 08028 Barcelona, Spain*

Abstract: This work presents the design of a three-layer control strategy to regulate the water levels in inland waterways. The upper layer takes into account the tidal period, which defines two different operating modes. A controller is designed for each mode in the intermediate layer, as well as an observer that estimates the states and the disturbances. Finally, the lower layer solves an optimization problem that yields the scheduling of a set of discrete actuators that best approximates the optimal reference. A real case study based on part of the inland waterways in the north of France is used to test the proposed approach and demonstrate its effectiveness.

Keywords: Inland waterways, model predictive control, moving horizon estimation, multi-layer architecture, discrete actuators.

1. INTRODUCTION

Inland waterways are large-scale systems composed of rivers and canals and used mainly for transportation of passengers and freight. Their management aims at allocating the available water resources to meet the desired objectives, the most important of which is to guarantee the navigability condition, i.e., ensure that the water levels are kept within a safety interval. Other common management objectives are oriented towards minimizing the operational cost and ensuring a long lifespan of the equipment.

Inland waterways are complex systems affected by complex phenomena, e.g., demand uncertainty, rainfall and seepage, which requires the use of advanced control techniques to fulfill the objectives. One of the most popular approaches is model predictive control (MPC), which employs a dynamic representation of the process subject to physical and operational restrictions to predict the effect of a set of controlled inputs, such that the plant performance is optimal with respect to the objectives (Rawlings and Mayne, 2009). Moreover, the use of an observer is often needed to provide the MPC with the system states, as these are generally not measurable. Among the existing options, moving horizon estimation (MHE), often considered as the dual problem of MPC, emerges as a natural choice. Their combination is indeed attractive since the MHE is also formulated as an online optimization problem that can explicitly handle constraints (Rao et al., 2001).

Given the inherently complex nature of inland waterways, designing the controller as a single entity with a centralized decision mechanism may not be reasonable. Instead, a common approach consists in decomposing the original task into a sequence of simpler and structured subtasks, each of them handled in a different layer (Tatjewski, 2008). In this way, the complexity of the control design can be reduced, and its reliability improved. This approach has been used in a large variety of applications such as autonomous vehicles (Falcone et al., 2008), power plants (Edlund et al., 2011) and polymerization processes (Würth et al., 2011). Concerning water systems, it has also been employed in irrigation canals (Zafra-Cabeza et al., 2011), municipal water networks (Ocampo-Martinez et al., 2014) and wastewater treatment processes (Santín et al., 2015).

Summary of the paper and contribution

This work proposes a multi-layer approach to regulate the water levels in inland waterways. The first steps were carried out in Segovia et al. (2019), where a control-oriented model belonging to the class of delayed descriptor systems was formulated. Moreover, MPC and MHE were employed for control and state estimation. However, the proposed strategy assumed perfectly known disturbances, it did not take into account the tidal periods and neither did it consider discrete actuators to apply the optimal references. Conversely, this work proposes a multi-layer design that allows to make use of the aforementioned previous results while tackling these three new issues.

The rest of the paper is organized as follows: Section 2 features the problem statement. The proposed approach is described in Section 3. The case study and the results are featured in Section 4, which allows to draw conclusions and outline future steps in Section 5.

2. PROBLEM STATEMENT

Inland waterways management is concerned with regulating the levels of the canals so that these are kept within the navigation rectangle, i.e., an interval around the normal navigation level (NNL). Moreover, an optimal dispatch of the water resources is of the utmost importance, especially in a context of climate change. Oftentimes however, certain phenomena oppose the attainment of the objectives, such as the operation of locks to allow the navigation of vessels, which cannot be scheduled in an optimal manner and thus result in undesired water flows, and the existence of uncontrolled inflows and outflows along the water course.

In addition to rejecting disturbances, the strategies need to take into account additional aspects at the design stage. In certain scenarios such as the case study considered in this work, canals are used to dispatch the excess of water in crop fields to the sea. To do so, pumping stations and gates are installed at the downstream end of the canal and operated to fulfill the management objectives. Nevertheless, sea tides must be taken into account, as the use of gates is usually not permitted in lowlands during high tide periods for safety reasons. These periods correspond to the situations in which the sea level is higher than the canal level. Thus, two operating modes can be defined, one for high tide and another for low tide, and a controller is to be designed for each mode.

Finally, the low-level control is also dealt with in this work. Consider that the aforementioned controllers provide an optimal set of references that must be sent to the local slave controllers, which in turn must ensure that the actuators supply the desired flows. However, pumping stations often consist in a set of binary devices, i.e., each pump in the station either supplies its design flow or is not operated. Thus, pumping stations are usually unable to supply the exact optimal value. A possible solution consists in scheduling the activation of the pumps such that their combined effect minimizes the error with respect to the optimal reference. On the other hand, gates can be generally operated with a higher degree of finesse.

In view of the above, a multi-layer scheme is proposed:

- The *upper* layer determines the tidal period.
- The *intermediate* layer solves the corresponding MPC (according to the tide), providing the optimal references to the local slave controllers. An MHE is also solved to estimate the states and the disturbances.
- The *lower* layer solves another optimization problem that yields the scheduling of the pumps that best approximates the given optimal references.

The design of each layer is carried out in the next section.

3. PROPOSED APPROACH

3.1 Upper layer

The upper layer must determine whether it corresponds to a high or a low tide period. As it was mentioned before, gates cannot be used during high tide in lowlands due to safety reasons. This behavior establishes two different operating modes, which result in two different controllers, one for each situation. Therefore, it is crucial to determine each period effectively, which can be done by comparing the sea level with the canal level: a sea level higher than the canal level corresponds to a high tide period, and vice versa. A possible way to circumvent the lack of information regarding the sea level is to consider one of the three basic tidal patterns (Pugh and Woodworth, 2014):

- *Semidiurnal* tides are characterized by two high and two low tides every day, each of them lasting about six hours. The heights of the two highs and the two lows are approximately the same.
- *Mixed semidiurnal* tides follow the same pattern, but the two highs and lows differ in height.
- *Diurnal* tides only have one high and one low tide each day, each of them lasting about twelve hours.

3.2 Intermediate layer

An MPC coupled to an MHE is designed in the intermediate layer to compute the set of optimal references. Their design is adapted from Segovia et al. (2019), where the reader is referred to check the complete derivation.

The low tide MPC is formulated as follows:

$$\min_{\substack{\left\{\mathbf{u}^g_{i|k}\right\}_{i=k}^{k+H_p-1},\ \left\{\mathbf{u}^p_{i|k}\right\}_{i=k}^{k+H_p-1},\\ \left\{\mathbf{y}_{i|k}\right\}_{i=k}^{k+H_p-1},\ \left\{\boldsymbol{\alpha}_{i|k}\right\}_{i=k}^{k+H_p-1}}} J\left(\mathbf{u}^g_{i|k}, \mathbf{u}^p_{i|k}, \mathbf{y}_{i|k}, \boldsymbol{\alpha}_{i|k}\right) \quad (1)$$

subject to:

$$\begin{aligned}
\mathbf{x}_{i+1|k} &= \mathbf{A}\mathbf{x}_{i|k} + \mathbf{B}^g_u\mathbf{u}^g_{i|k} + \mathbf{B}^p_u\mathbf{u}^p_{i|k} + \mathbf{B}^g_{un}\mathbf{u}^g_{i-n|k} + \\
&\quad \mathbf{B}^p_{un}\mathbf{u}^p_{i-n|k} + \mathbf{B}_d\mathbf{d}_{i|k} + \mathbf{B}_{dn}\mathbf{d}_{i-n|k}, \\
&\quad i \in \{k, ..., k+H_p-1\}, \\
\mathbf{y}_{i|k} &= \mathbf{C}\mathbf{x}_{i|k} + \mathbf{D}^g_u\mathbf{u}^g_{i|k} + \mathbf{D}^p_u\mathbf{u}^p_{i|k} + \mathbf{D}^g_{un}\mathbf{u}^g_{i-n|k} + \\
&\quad \mathbf{D}^p_{un}\mathbf{u}^p_{i-n|k} + \mathbf{D}_d\mathbf{d}_{i|k} + \mathbf{D}_{dn}\mathbf{d}_{i-n|k}, \\
&\quad i \in \{k, ..., k+H_p-1\}, \\
\mathbf{0} &= \mathbf{E}^g_u\mathbf{u}^g_{i|k} + \mathbf{E}^p_u\mathbf{u}^p_{i|k} + \mathbf{E}^g_{un}\mathbf{u}^g_{i-n|k} + \mathbf{E}^p_{un}\mathbf{u}^p_{i-n|k} + \\
&\quad \mathbf{E}_d\mathbf{d}_{i|k} + \mathbf{E}_{dn}\mathbf{d}_{i-n|k},\ i \in \{k, ..., k+H_p-1\}, \\
\underline{\mathbf{u}}^g &\le \mathbf{u}^g_{i|k} \le \overline{\mathbf{u}}^g,\ i \in \{k, ..., k+H_p-1\}, \\
\underline{\mathbf{u}}^p &\le \mathbf{u}^p_{i|k} \le \overline{\mathbf{u}}^p,\ i \in \{k, ..., k+H_p-1\}, \\
\underline{\mathbf{y}} - \boldsymbol{\alpha}_{i|k} &\le \mathbf{y}_{i|k} \le \overline{\mathbf{y}} + \boldsymbol{\alpha}_{i|k},\ i \in \{k, ..., k+H_p-1\}, \\
\boldsymbol{\alpha}_{i|k} &\ge \mathbf{0},\ i \in \{k, ..., k+H_p-1\}, \\
\mathbf{x}_{j|k} &= \hat{\mathbf{x}}^{MHE}_j,\ j \in \{k-n, ..., k\}, \\
\mathbf{d}_{j|k} &= \hat{\mathbf{d}}^{MHE}_j,\ j \in \{k-n, ..., k\}, \\
\mathbf{u}^g_{l|k} &= \mathbf{u}^{MPC(g)}_l,\ l \in \{k-n, ..., k-1\}, \\
\mathbf{u}^p_{l|k} &= \mathbf{u}^{MPC(p)}_l,\ l \in \{k-n, ..., k-1\},
\end{aligned}$$

where $\mathbf{x}_k \in \mathbb{R}^{n_x}$ are the states, $\mathbf{y}_k \in \mathbb{R}^{n_y}$ are the levels, $\mathbf{u}^g_k \in \mathbb{R}^{n_{ug}}$ and $\mathbf{u}^p_k \in \mathbb{R}^{n_{up}}$ are the total gate and pumping control actions, respectively, $\mathbf{d}_k \in \mathbb{R}^{n_d}$ are the disturbances, $\boldsymbol{\alpha}_k \in \mathbb{R}^{n_y}$ is a relaxation parameter, H_p is the prediction horizon and the multi-objective cost function J is the same as in Segovia et al. (2019), thus penalizing tracking errors, noncompliance of the navigability condition, control effort and non-smooth control signals. Moreover, $k \in \mathbb{Z}_{\ge 0}$ is the current time instant, $i \in \mathbb{Z}_{\ge 0}$ is the time instant along the prediction horizon, $k+i|k$ indicates the predicted value of the variable at instant

$k+i$ using information available at instant k, and $j \in \mathbb{Z}_{\geq 0}$ and $l \in \mathbb{Z}_{\geq 0}$ indicate the use of past information already computed by the MPC or MHE (denoted by means of superscripts), for which the considered time intervals are different than the one described by i.

Remark 1. The high tide MPC can be obtained from (1) by eliminating the variables $\mathbf{u}^g_{i|k}$ and $\mathbf{u}^g_{i-n|k}$. □

The optimal solution is given by the sequences $\{\mathbf{u}^g_{i|k}\}_{i=k}^{k+H_p-1}$, $\{\mathbf{u}^p_{i|k}\}_{i=k}^{k+H_p-1}$, $\{\mathbf{y}_{i|k}\}_{i=k}^{k+H_p-1}$ and $\{\boldsymbol{\alpha}_{i|k}\}_{i=k}^{k+H_p-1}$[1]. However, only $\mathbf{u}^g_{k|k} \in \mathbb{R}_{\geq 0}$ and $\mathbf{u}^p_{k|k} \in \mathbb{R}_{\geq 0}$ need to be provided to the lower layer, according to the receding philosophy $\mathbf{u}_k^{MPC(g)} \triangleq \mathbf{u}^g_{k|k}$ and $\mathbf{u}_k^{MPC(p)} \triangleq \mathbf{u}^p_{k|k}$.

On the other hand, the states $\hat{\mathbf{x}}_j^{MHE}$ and the disturbances $\hat{\mathbf{d}}_j^{MHE}$ are obtained as the solution of the MHE:

$$\min_{\substack{\{\hat{\mathbf{x}}_{i|k}\}_{i=k-N+1}^{k+1} \\ \{\hat{\mathbf{d}}_{i|k}\}_{i=k-N+1}^{k}}} \mathbf{w}^\intercal_{k-N+1|k}\mathbf{P}^{-1}\mathbf{w}_{k-N+1|k} + \sum_{i=k-N+1}^{k}\left(\mathbf{w}^\intercal_{i|k}\mathbf{Q}^{-1}\mathbf{w}_{i|k} + \mathbf{v}^\intercal_{i|k}\mathbf{R}^{-1}\mathbf{v}_{i|k}\right) \tag{2}$$

subject to:

$$\mathbf{w}_{k-N+1|k} = \hat{\mathbf{x}}_{k-N+1|k} - \mathbf{x}_{k-N+1},$$
$$\mathbf{w}_{i|k} = \hat{\mathbf{x}}_{i+1|k} - \Big(\mathbf{A}\hat{\mathbf{x}}_{i|k} + \mathbf{B}^g_u\mathbf{u}^g_{i|k} + \mathbf{B}^p_u\mathbf{u}^p_{i|k} + \mathbf{B}^g_{un}\mathbf{u}^g_{i-n|k} + \mathbf{B}^p_{un}\mathbf{u}^p_{i-n|k} + \mathbf{B}_d\hat{\mathbf{d}}_{i|k} + \mathbf{B}_{dn}\hat{\mathbf{d}}_{i-n|k}\Big),\ i \in \{k-N+1,...,k\},$$
$$\mathbf{v}_{i|k} = \mathbf{y}_{i|k} - \Big(\mathbf{C}\hat{\mathbf{x}}_{i|k} + \mathbf{D}^g_u\mathbf{u}^g_{i|k} + \mathbf{D}^p_u\mathbf{u}^p_{i|k} + \mathbf{D}^g_{un}\mathbf{u}^g_{i-n|k} + \mathbf{D}^p_{un}\mathbf{u}^p_{i-n|k} + \mathbf{D}_d\hat{\mathbf{d}}_{i|k} + \mathbf{D}_{dn}\hat{\mathbf{d}}_{i-n|k}\Big),\ i \in \{k-N+1,...,k\},$$
$$\mathbf{0} = \mathbf{E}^g_u\mathbf{u}^g_{i|k} + \mathbf{E}^p_u\mathbf{u}^p_{i|k} + \mathbf{E}^g_{un}\mathbf{u}^g_{i-n|k} + \mathbf{E}^p_{un}\mathbf{u}^p_{i-n|k} + \mathbf{E}_d\hat{\mathbf{d}}_{i|k} + \mathbf{E}_{dn}\hat{\mathbf{d}}_{i-n|k},\ i \in \{k-N+1,...,k\},$$
$$\mathbf{y}_{i|k} = \mathbf{y}_i,\ i \in \{k-N+1,...,k\},$$
$$\hat{\mathbf{d}}_{i|k} \geq \mathbf{0},\ i \in \{k-N+1,...,k\},$$
$$\underline{\mathbf{x}} \leq \hat{\mathbf{x}}_{j|k} \leq \overline{\mathbf{x}},\ j \in \{k-N+1,...,k+1\},$$
$$\hat{\mathbf{x}}_{l|k} = \hat{\mathbf{x}}_l^{MHE},\ l \in \{k-N-n+1,...,k-N\},$$
$$\hat{\mathbf{d}}_{l|k} = \hat{\mathbf{d}}_l^{MHE},\ l \in \{k-N-n+1,...,k-N\},$$
$$\mathbf{u}^g_{m|k} = \mathbf{u}_m^{MPC(g)},\ m \in \{k-N-n+1,...,k\},$$
$$\mathbf{u}^p_{m|k} = \mathbf{u}_m^{MPC(p)},\ m \in \{k-N-n+1,...,k\},$$

where N is the length of the window, $\mathbf{P}^{-1}$, $\mathbf{Q}^{-1}$ and $\mathbf{R}^{-1}$ are the weighting matrices, $\mathbf{x}_{k-N+1}$ corresponds to the most likely initial state and $\mathbf{y}_i$ are the measured levels.

Problem (2) is solved, yielding the optimal sequences $\{\hat{\mathbf{x}}_{i|k}\}_{i=k-N+1}^{k+1}$ and $\{\hat{\mathbf{d}}_{i|k}\}_{i=k-N+1}^{k}$. However, as is the case in the MPC problem, only one value in the sequence is considered, and the rest are discarded. In the MHE, this corresponds to the last value of the sequences. Therefore, $\hat{\mathbf{x}}_k^{MHE} \triangleq \hat{\mathbf{x}}_{k+1|k}$ and $\hat{\mathbf{d}}_k^{MHE} \triangleq \hat{\mathbf{d}}_{k|k}$.

[1] $\{\mathbf{u}^g_{i|k}\}_{i=k}^{k+H_p-1} \triangleq \{\mathbf{u}^g_{k|k}, \mathbf{u}^g_{k+1|k}, \cdots, \mathbf{u}^g_{k+H_p-1|k}\}$; $\mathbf{u}^p_{i|k}$, $\mathbf{y}_{i|k}$ and $\boldsymbol{\alpha}_{i|k}$ are defined in the same manner

3.3 Lower layer

The final task consists in determining the set of activation states of the pumps that approximates best the optimal references computed by the MPC. It is recalled that both gates and pumping stations are considered to be installed in the system. In this work, gates are assumed to be able to supply the exact flow, whereas pumps are modeled as on/off actuators. Therefore, the lower layer is only concerned with the scheduling of the pumps, which is obtained as the solution of the following problem for each pumping station:

$$\min_{\left\{\mathbf{s}^j_{i|k}\right\}_{i=k}^{k+M-1}} \gamma_1 \left\| T_{s_1} u_k^{MPC(p_j)} - T_{s_2} \sum_{i=k}^{k+M-1}\sum_{l=1}^{n_{p_j}} u_d^{p_j}(l) s_i^j(l) \right\|_2 + \gamma_2 \left(\Delta\mathbf{s}_i^j\right)^\intercal \Delta\mathbf{s}_i^j \tag{3}$$

subject to:

$$s_i^j(l) \in \{0,1\},\ i \in \{k,...,k+M-1\},\ l \in \{1,...,n_{p_j}\},$$
$$s_i^j(l+1) + \left(1 - s_i^j(l)\right) \leq 1,\ i \in \{k,...,k+M-1\},\ l \in \{1,...,n_{p_j}-1\},$$

where i indicates the time instant, j identifies the pumping station and l indexes the position of the pump within the pumping station. Moreover, n_{p_j} is the number of pumps in the j-th pumping station, $u_k^{MPC(p_j)}$ is the j-th component of the optimal pumping action provided by the MPC, $\mathbf{s}_i^j$ is the vector of activation states of the j-th pumping station at time instant i, $u_d^{p_j}(l)$ is the design flow of the l-th pump at the j-th pumping station and $M = T_{s_1}/T_{s_2}$ is the total number of pumping instants within two consecutive solutions provided by the MPC. Indeed, it is assumed that both the upper and the intermediate layer work with a sampling time T_{s_1}, whereas the lower layer works with a sampling time T_{s_2}, with $T_{s_2} < T_{s_1}$, and T_{s_2} is chosen such that $\text{mod}(T_{s_1}, T_{s_2}) = 0$.

Note that it is also desirable that the optimal scheduling minimizes the number of activation state switchings, which is formulated as an additional objective in the cost function. The relative importance of the two objectives is weighted by means of the coefficients γ_1 and γ_2.

Remark 2. $s_i^j(l) = 0$ means that the l-th pump at the j-th station is switched off at instant i, and vice versa. □

Therefore, the solution of the lower layer consists in a sequence of on/off states for each pump at each pumping station. The second constraint in (3), which follows the ideas presented in Galindo et al. (2017), ensures a sequential order in the activation of the pumps. Indeed, it is required that the first pump is on before the second pump can be switched on, and so on.

3.4 Simulation of the multi-layer approach

The proposed approach is implemented and simulated as shown in Algorithm 1. Note that the simulation loop is executed using the low-level layer sampling time T_{s_2}. On the other hand, the MPC and the scheduling problem are

Algorithm 1 Design of the simulation loop

Require: parameters in problems (1), (2) and (3)

Estimate $\hat{\mathbf{x}}_0$ and $\hat{\mathbf{d}}_0$
Set $\hat{\mathbf{x}}^{MHE} = \hat{\mathbf{x}}_0$ and $\hat{\mathbf{d}}^{MHE} = \hat{\mathbf{d}}_0$
for $k = 0 : t_{sim}$ **do**
  if $\mathrm{mod}(k, M) = 0$ **then**
    Adapt MPC controller according to tidal period
    Solve (1) using $\hat{\mathbf{x}}^{MHE}$ and $\hat{\mathbf{d}}^{MHE}$
    Extract $\mathbf{u}^{MPC(g)}$ and $\mathbf{u}^{MPC(p)}$ from solution
    Solve (3) using $u^{MPC(p_j)}$, $\forall j \in \{1, 2, \cdots, n_j\}$
    Obtain n_j activation sequences $\mathbf{s}^j$
  end if
  Set $\mathbf{u}_k^{(g)} = \frac{1}{M}\mathbf{u}^{MPC(g)}$
  Set $u_k^{(p_j)} = \sum_{l=1}^{n_{p_j}} u_d^{p_j}(l) s_r^j(l)$, with $r = \mathrm{mod}(k, M)$ and $\forall j \in \{1, 2, \cdots, n_j\}$
  Build $\mathbf{u}_k^{(p)} = \left[u_k^{(p_1)}, u_k^{(p_2)}, \cdots, u_k^{(p_{n_j})}\right]^\intercal$
  Apply $\mathbf{u}_k^{(g)}$ and $\mathbf{u}_k^{(p)}$ to the system
  if $\mathrm{mod}(k, M) = M - 1$ **then**
    Set $\mathbf{u} = \sum_{r=k-M+1}^{k} \mathbf{u}_r$
    Measure $\mathbf{y}$
    Solve (2) using the N last $(\mathbf{u}, \mathbf{y})$ pairs
    Extract $\hat{\mathbf{x}}^{MHE}$ and $\hat{\mathbf{d}}^{MHE}$ from solution
  end if
end for

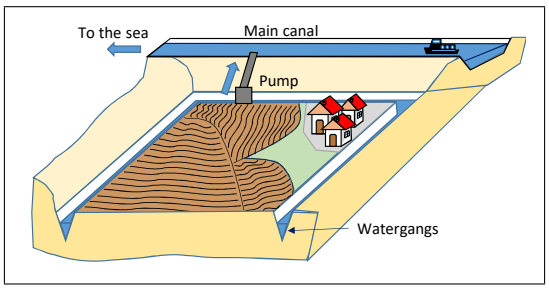

Fig. 1. Schematic representation of part of the Wateringues, taken from Duviella and Hadid (2019)

executed only every M samples, which corresponds to T_{s_1} seconds. Thus, a set of M pumping actions are obtained and sequentially applied in the next M instants. Their total effect is measured after the M instants to solve the MHE problem and obtain the new set of estimates that are used in the next iteration by the MPC.

4. CASE STUDY: THE CALAIS CANAL

4.1 System description

The Calais canal is a navigation canal located in the Wateringues territory in the north of France. These areas, also known as polders, consist in maritime plains below the sea level in which water is collected by means of ditches known as watergangs. The excess of water in the watergangs is pumped to the navigation canals and then released into the sea. A schematic representation of these systems is depicted in Fig. 1.

The system of study consists in a main canal supplied by three secondary canals. Its physical data is summarized

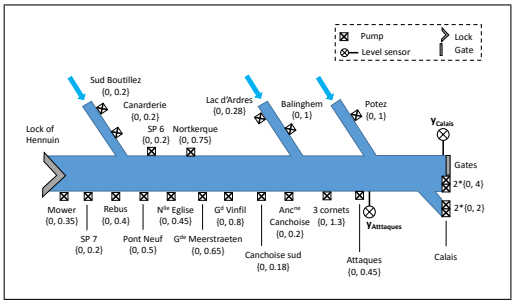

Fig. 2. Schematic representation of the Calais canal, adapted from Duviella and Hadid (2019)

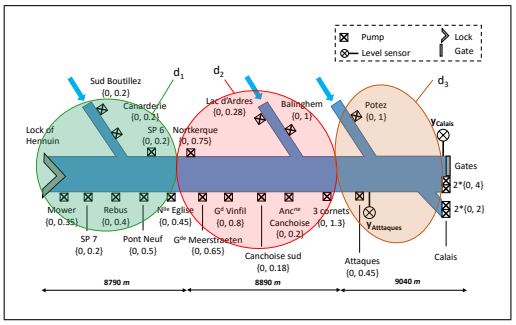

Fig. 3. Schematic representation with pumping actions grouped, adapted from Duviella and Hadid (2019)

in Table 1. The canal is bounded at the upstream end by the lock of Hennuin, and by sea outlet gates and a pumping station equipped with four pumps at the downstream end, which are used to regulate the levels. The management policy promotes using the gate over the pumps whenever it is possible. In addition, eighteen pumps used to dispose of the excess of water in the watergangs are installed along the canal, which are manipulated by the farmers at their convenience and are thus regarded as disturbances. Moreover, two level sensors allow to obtain level measurements in Attaques and Calais. A schematic view of the canal is depicted in Fig. 2, including the design flow of each pump. Then, for the sake of simplicity, and following the strategy defined by Duviella and Hadid (2019), the eighteen pumps are grouped into d_1, d_2 and d_3 as shown in Fig. 3.

The management objectives consist in keeping the water levels in Attaques and Calais within the interval [LNL, HNL] specified in Table 1. These levels are disturbed by the unpredictable operation of the eighteen pumps, which result in the disturbances d_1, d_2 and d_3 depicted in Fig. 3. The actuators in Calais are operated as specified in Sections 2 and 3 to reject these disturbances.

4.2 Experimental design

The water levels are disturbed considering the signals in Fig. 4 to test the proposed approach. These disturbances are injected in a model built in SIC^2, a hydraulic simulation software (Malaterre and Baume, 1997), as it is not possible to access the real system. Moreover, as the historical record of the sea level is not available, a semidiurnal tidal pattern is considered, given the canal location.

On the other hand, the model upon which the MPC and MHE are designed is obtained as detailed in Segovia et al.

Table 1. Physical data of the Calais canal

LNL $[m]$	NNL $[m]$	HNL $[m]$	Length $[m]$	Width $[m]$	Side slope $[m/m]$	Bottom slope $[m/m]$	Manning coeff. $[s/m^{1/3}]$	Average flow $[m^3/s]$
2.1	2.2	2.35	26720	20	0	0	0.035	1

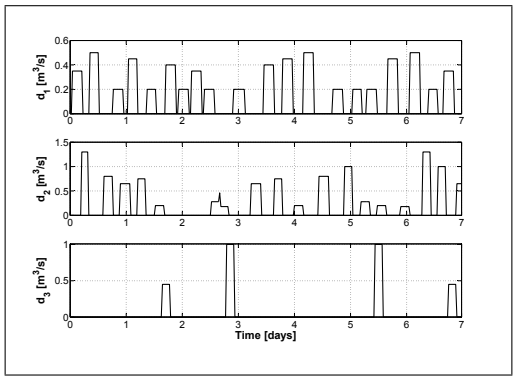

Fig. 4. Considered disturbance scenario

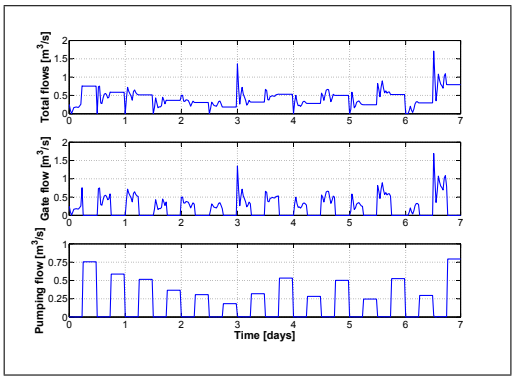

Fig. 6. Optimal flows computed by the MPC

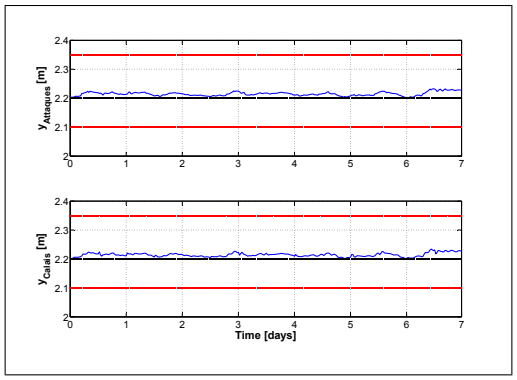

Fig. 5. Water levels (blue solid line), NNL (black dashed line), and LNL and HNL (red dashed line)

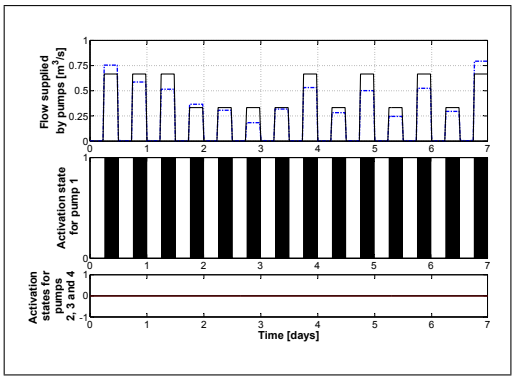

Fig. 7. Solution of the scheduling problem

(2019) and implemented in MATLAB® using YALMIP (Löfberg, 2004). Both H_p in (1) and N in (2) are chosen equal to twelve hours to consider high and low tide periods, with T_{s_1} and T_{s_2} equal to 30 and 5 minutes, respectively. Then, the simulation is performed as stated in Algorithm 1, with SIC^2 and MATLAB® exchanging information.

4.3 Results

The evolution of the water levels is depicted in Fig. 5, showing that the levels never cross the boundaries, and thus the control strategy performs as desired. Moreover, the error between the water levels and the references can be quantified using the following indices:

$$TP = 1 - \frac{1}{t_{sim}} \sqrt{\sum_{k=1}^{t_{sim}} \left(\frac{y_k - NNL}{\frac{1}{2}\left(\overline{y} - \underline{y}\right)} \right)^2}, \qquad (4)$$

which are equal to 0.9974 for Attaques and 0.9973 for Calais and allow to highlight the satisfactory performance of the control strategy.

Figure 6 depicts the solution of the MPC, i.e., the optimal flows that must by supplied by the gate and the pumps, as well as their combined action. These values are far from the limits (14.7 and 12 m^3/s, respectively), which are not depicted for the sake of a better visualization. Note that the pumps are barely used during low tide (aligned with the policy described in Section 4.1), whereas the gate is not operated during high tide for safety reasons.

The results pertaining to the lower layer are depicted in Fig. 7. The first subplot shows the optimal flow computed by the MPC (dashed blue line) and the approximation obtained after solving the scheduling problem (black solid line). Note that two factors affect the degree of accuracy of the discrete solution with respect to the optimal values: the magnitude of the design flows and the rate of setpoint variation. Indeed, the smaller the design flows and the variation rates are, the closer the intermediate and the lower layer control solutions are. On the other hand, the second and third subplots show the activation states of the four pumps, which are allowed to change every five minutes, although their variation is penalized. Therefore, the presented solution is obtained as a trade-off between the two objectives that are to be fulfilled. Furthermore, it can be realized that only one pump is needed to supply the flow, thus complying with the specifications given in Section 3.3. Note that the signal in the second subplot allows to obtain the black solid signal in the first subplot.

Finally, the optimal gate actions, the scheduling of the pumps and the measured water levels allow to solve the MHE. Both the state estimates and the states computed using the simplified model are depicted in Fig. 8. Moreover, the similarity of both signals is quantified using the correlation coefficient: given a pair of signals (m, n) with L observations each, this coefficient is defined as

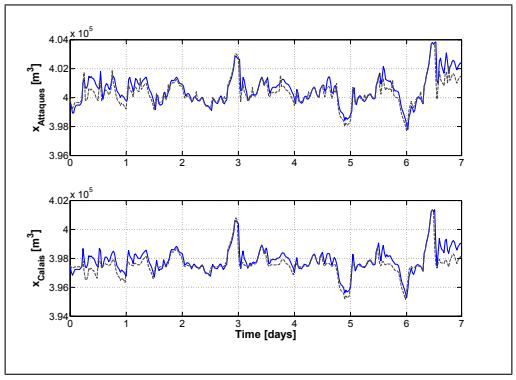

Fig. 8. State estimates (blue solid line) and computed states (gray dashed line)

$$\rho_{m,n} = \frac{1}{L-1}\sum_{i=1}^{L}\left(\frac{m_i-\mu_m}{\sigma_m}\right)\left(\frac{n_i-\mu_n}{\sigma_n}\right), \qquad (5)$$

where (μ_m, σ_m) and (μ_n, σ_n) are the mean and standard deviation of m and n, respectively. These coefficients are equal to 0.9586 for Attaques and 0.9536 for Calais, which allows to highlight its satisfactory performance.

5. CONCLUSIONS

This work has presented the design of a multi-layer control approach for the regulation of inland waterways. Three layers have been considered to solve the problem: the upper layer provides information regarding the tidal period, which defines two operating modes that are taken into account in the definition of the controllers at the intermediate layer level. An additional observer estimates the unmeasurable states and the disturbances affecting the system. Finally, the lower layer solves another optimization problem, providing the scheduling of a set of binary actuators whose combined action approximates the optimal solution. A case study built upon a real system serves to test the approach and show its effectiveness.

The proposed strategy can be extended to consider larger portions of the real system. In this case, however, it could be useful to consider non-centralized approaches such as the one designed in Segovia et al. (2019) to improve the scalability and reliability. On the other hand, the occurrence and effect of faults in the system could be investigated. In this regard, the fault diagnosis scheme proposed in Segovia et al. (2018) could be used to reconfigure the controller, leading to a fault-tolerant control strategy.

ACKNOWLEDGEMENTS

This work has been supported by ARMINES through the contract 1908V/1700661, the Scientific Research Network on Integrated Automation and Human-Machine Systems (GIS GRAISyHM), the Regional Council of Hauts-de-France (Regional Council of Nord - Pas de Calais - Picardie from France) and the IIW (Institution Intercommunale des Wateringues). The authors gratefully acknowledge the support of these institutions.

REFERENCES

Duviella, E. and Hadid, B. (2019). Simulation tool of the Calais Canal implementing Logic Control based regulation. *IFAC-PapersOnLine*, 52(23), 23–28.

Edlund, K., Bendtsen, J., and Jørgensen, J. (2011). Hierarchical model-based predictive control of a power plant portfolio. *Control Engineering Practice*, 19(10), 1126–1136.

Falcone, P., Borrelli, F., Tseng, H., Asgari, J., and Hrovat, D. (2008). A hierarchical MPC framework for autonomous ground vehicles. In *2008 American Control Conference*, 3719–3724.

Galindo, J., Torok, S., Salguero, F., de Campos, S., Romera, J., and Puig, V. (2017). Optimal management of water and energy in irrigation systems: application to the Bardenas canal. *IFAC-PapersOnLine*, 50(1), 6613 – 6618.

Löfberg, J. (2004). YALMIP: a toolbox for modeling and optimization in MATLAB. In *IEEE International Symposium on Computer Aided Control Systems Design*.

Malaterre, P.O. and Baume, J.P. (1997). SIC 3.0, a simulation model for canal automation design. In *Int. Workshop on Regulation of Irrigation Canals*, 68–75.

Ocampo-Martinez, C., Puig, V., Grosso, J.M., and Montes de Oca, S. (2014). Multi-layer Decentralized MPC of Large-scale Networked Systems. In *Distributed Model Predictive Control Made Easy*, 495–515. Springer Netherlands, Dordrecht.

Pugh, D. and Woodworth, P. (2014). *Sea-level science: understanding tides, surges, tsunamis and mean sea-level changes*. Cambridge University Press.

Rao, C.V., Rawlings, J.B., and Lee, J.H. (2001). Constrained linear state estimation – a moving horizon approach. *Automatica*, 37(10), 1619–1628.

Rawlings, J.B. and Mayne, D.Q. (2009). *Model predictive control: theory and design*. Nob Hill Pub. Madison.

Santín, I., Pedret, C., and Vilanova, R. (2015). Applying variable dissolved oxygen set point in a two level hierarchical control structure to a wastewater treatment process. *Journal of Process Control*, 28, 40 – 55.

Segovia, P., Blesa, J., Horváth, K., Rajaoarisoa, L., Nejjari, F., Puig, V., and Duviella, E. (2018). Modeling and fault diagnosis of flat inland navigation canals. *Proc. of the Institution of Mechanical Engineers, Part I: Journal of Systems and Control Engineering*, 232(6), 761–771.

Segovia, P., Rajaoarisoa, L., Nejjari, F., Duviella, E., and Puig, V. (2019). A communication-based distributed model predictive control approach for large-scale systems. In *2019 IEEE 58th Conference on Decision and Control (CDC)*, 8366–8371.

Segovia, P., Rajaoarisoa, L., Nejjari, F., Duviella, E., and Puig, V. (2019). Model predictive control and moving horizon estimation for water level regulation in inland waterways. *Journal of Process Control*, 76, 1–14.

Tatjewski, P. (2008). Advanced control and on-line process optimization in multilayer structures. *Annual Reviews in Control*, 32(1), 71 – 85.

Würth, L., Hannemann, R., and Marquardt, W. (2011). A two-layer architecture for economically optimal process control and operation. *Journal of Process Control*, 21(3), 311 – 321.

Zafra-Cabeza, A., Maestre, J.M., Ridao, M.A., Camacho, E.F., and Sánchez, L. (2011). A hierarchical distributed model predictive control approach to irrigation canals: a risk mitigation perspective. *Journal of Process Control*, 21(5), 787–799.